Stark Effect on Single Molecules of Dibenzanthanthrene in a Naphthalene Crystal and in a n-Hexadecane Shpol'skii Matrix

ARTICLE *in* THE JOURNAL OF PHYSICAL CHEMISTRY A · MARCH 1999

Impact Factor: 2.69 · DOI: 10.1021/jp983956t

Stark Effect on Single Molecules of Dibenzanthanthrene in a Naphthalene Crystal and in a *n*-Hexadecane Shpol'skii Matrix

Ch. Brunel, Ph. Tamarat, B. Lounis, J. C. Woehl, and M. Orrit*

Centre de Physique Moléculaire Optique et Hertzienne, CNRS et Université Bordeaux I, 351 Cours de la Libération, 33405 Talence, France

Received: October 5, 1998; In Final Form: December 8, 1998

We investigated the Stark effect on centrosymmetric dibenzanthanthrene molecules in naphthalene, a centrosymmetric crystal, where it is mainly quadratic, and in the Shpol'skii matrix hexadecane, where we found linear and quadratic contributions. The molecules with large linear coefficients are dominantly found in the wings of the main site. The distribution of linear coefficients points to two populations of molecules, one of them in a centrosymmetric environment, the other one centrosymmetric on average, but very sensitive to, or located near, crystal defects. The distributions of quadratic coefficients in both systems is attributed to orientational disorder. We discuss the case of a molecule with higher-order terms in its Stark shift, and attribute it to geometrical changes of the supermolecule in the applied electric field.

1. Introduction

Electrochromism[1] is the change in the electronic spectra of matter under an applied electric field. It is related to the Stark effect, i.e., to the electric field-induced shift of the electronic levels of atoms, molecules, or solids. Electrochromism gives information about the static dipole moments and polarizabilities of molecules, more precisely about the difference of these quantities between the ground and excited electronic states involved in the optical absorption. The electric fields that can be applied to solid or liquid samples being limited by dielectric break-down, are much weaker than internal molecular or crystal fields. Therefore, the electrochromism of the broad bands of molecular systems at room temperature is a weak effect. It must be measured by modulating the applied field and detecting the absorption change with a lock-in amplifier at the modulation frequency (linear effect) or at twice the modulation frequency (quadratic effect).[2] The narrower the optical band is, the stronger the electrochromic signal. Electric field effects are therefore easier to measure on the narrow zero-phonon lines of molecular crystals[3] or of solutes in Shpol'skii matrixes at cryogenic temperatures.

The spectral resolution in optical investigations of organic molecular systems can be enormously enhanced by the technique of persistent spectral hole burning.[4,5] Since narrow spectral holes are extremely sensitive to electric fields, electrochromism can be measured with 10^3-10^5 times higher sensitivity than in broad band spectra.[6−8] Spectral holes as narrow as a few MHz have been measured by the late B. E. Kohler and co-workers. The enhanced sensitivity in the measurement of the hole shift and broadening as functions of the electric field enabled them to develop a quantum mechanical approach to analyze the data for octatetraene in *n*-alkane matrixes[9] and for porphyrin chromophores in proteins such as myoglobin or cytochrome C.[10] Later, they even proposed a detailed modeling of the microscopic structure of the guest molecule and of its first two host shells with their charges.[11] The resulting internal field was found to be extremely inhomogeneous over the size of the guest molecule.

However, the hole signal arises from a large set of molecules, the isochromat, that all happen to have the same transition frequency for zero applied electric field. The molecules in the isochromat still present differences in their orientations and environments, and as a consequence, in their Stark effect parameters. Therefore, spectral holes quickly broaden for high fields and can no longer be measured accurately.[12] By isolating single molecules in spectra of solid solutions at low temperatures, one removes inhomogeneity completely. It is then possible to apply very high fields, without any broadening of the single molecule's signal. As a further advantage, the electrochromism of a single molecule is much easier to interpret than that of a spectral hole. One basically measures the shift $\delta\nu$ of the transition frequency of the molecule. At the lowest order in the electric field E acting on the molecule, the shift has linear and quadratic dependences in E:

$$\delta\nu = aE + bE^2 \tag{1}$$

where a and b are defined for each molecule, and for a given direction of the electric field with respect to the molecular axes. These coefficients are related to the dipole moment change $\delta\vec{\mu}$ and to the change of the polarizability tensor $\delta\bar{\bar{\alpha}}$ between ground and excited states of the molecule by

$$h\delta\nu = -\delta\vec{\mu}\cdot\vec{E} - \vec{E}\,\delta\bar{\bar{\alpha}}\,\vec{E}/2 \tag{2}$$

The field $\vec{E}$ acting on the molecule is the local field, i.e., the part of the true microscopic field which is linear in the applied external field.[13] In an isotropic medium, and for a point dipole, the local field is simply related to the macroscopic field in the medium by the Lorentz correction factor. Local field corrections in real systems are much more complex, since they must account for the anisotropy and the inhomogeneity of the microscopic field. In the following, we consider only Lorentz corrections.

Of course, higher order terms are expected to arise in eq 1, via higher order hyperpolarizabilities.[14] However, a crude

* Corresponding author.

10.1021/jp983956t CCC: $18.00
Published on Web 03/02/1999

estimation of the next, cubic, term in $\delta\nu$, which is related to the change in the second-order polarizability $\chi^{(2)}$, shows that it should be smaller than the quadratic term by a factor $r = E/E_{mol}$,[15] where E is the applied electric field strength and E_{mol} is a typical intramolecular field acting on the pi electron. The ratio r being typically less than 10^{-3}, third-, and higher order corrections are usually neglected in the analysis of the Stark effect.

The first Stark effect measurements on single molecules were performed in 1992 by Wild et al.[16] on pentacene in a *p*-terphenyl crystal. Since the pentacene molecule is centrosymmetrical and occupies a centrosymmetrical site in the p-terphenyl crystal, the Stark effect observed on single molecules in the O_1 and O_2 sites is dominantly quadratic for fields lower than 2.5 MV/m, with b coefficients of about 4 MHz/(MV/m)^2, corresponding to polarizability changes around 2×10^{-39} F m^2 (i.e., 20 Å^3; 1 Å^3 $= 1.11 \times 10^{-40}$ F m^2). The linear *a* coefficients found were very weak, about 1 MHz/(MV/m), corresponding to dipole moment changes from about 6 10^{-36} C m to about 1.5×10^{-33} C m (i.e., a few μD to 0.5 mD; 1 D $= 3.34 \times 10^{-30}$ C m). These weak values of the dipole moment were attributed to slight breaking of the molecular symmetry by crystal defects. The same year, Orrit et al.[17] investigated the Stark effect of terrylene in polyethylene. There, the centrosymmetry of the terrylene molecule was strongly broken by the disordered polymer matrix, leading to a purely linear Stark effect in the range of fields investigated (less than 0.1 MV/m). The absolute values of the a coefficients were about 3×10^3 MHz/(MV/m), corresponding to matrix-induced differences in dipole moments of about 0.5 D. More recently, Stark experiments were performed on single terrylene molecules in a *p*-terphenyl crystal.[18] As in the case of pentacene, the molecular centrosymmetry seems to be largely preserved in the X_1 site,[19] and the quadratic effect dominates.

Here, we present Stark effect measurements on single molecules of dibenzanthanthrene (DBATT) in naphthalene crystals[20] and in n-hexadecane Shpol'skii matrixes,[21] two systems studied recently in our group. By comparing our data to those published for other systems, we try to get information about the nature and symmetry of the insertion site and its sensitivity to defects. We also discuss deviations from the simple expression 1, which might arise from geometrical changes of the molecule or of its cage under the applied field.

2. Experimental Setup

The samples of DBATT in naphthalene were prepared from the melt, where the solubility of DBATT is high. The molten solution was rapidly cooled by contact with the optical fiber used for excitation (see Figure 1). A thin glass sheet was placed on the sample to prevent sublimation during handling. The polycrystal thus obtained presented an inhomogeneous band profile similar to that published in ref 20, with a width of about 12 cm^{-1}. The many defects in this highly disordered sample did not lead to any noticeable spectral diffusion of the single molecule lines. The hexadecane solution of DBATT was quickly frozen by inserting the sample holder into the cold cryostat. This resulted also in a polycrystalline sample, but the crystallite size is unknown. The optical setup for the fluorescence excitation spectroscopy of single molecules was of the fiber-paraboloid type.[22] We did not use the frequency stabilization of the laser for the present study.

The electrodes through which the electric field was applied are schematically represented in Figure 1. Two thin gold wires (20 μm in diameter) were flattened and fixed with epoxy glue

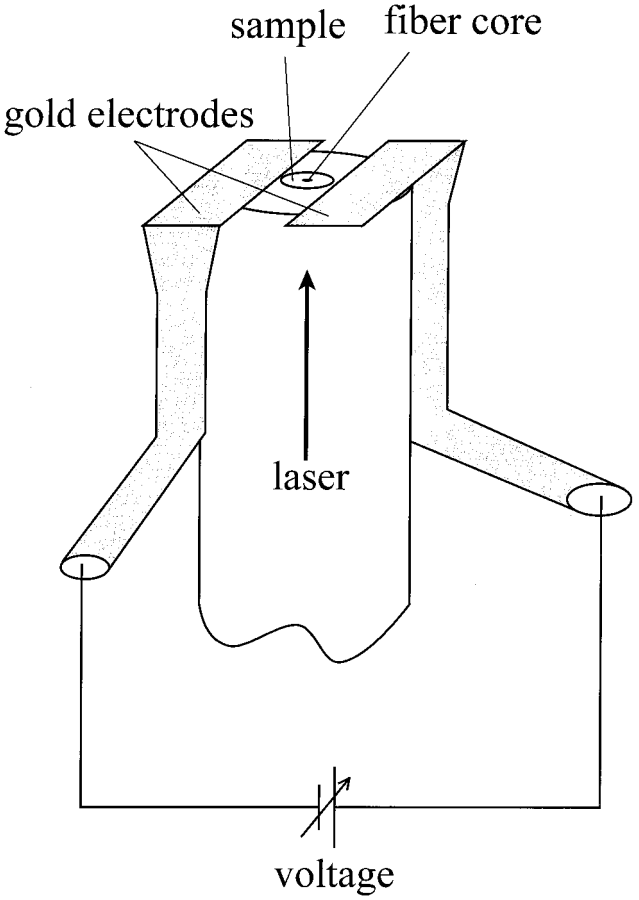

Figure 1. Schematic view of the end of the optical fiber with the gold electrodes to apply a static electric field. The sample has been placed on the fiber core, where the excitation light propagates.

at the end of the fiber on either side of the optical fiber core. The distance between electrodes was 25 ± 5 μm. The electric field at the sample was calculated by dividing the applied voltage by the distance between electrodes and by applying a correction factor of 0.64 to take the electrode geometry into account.[23] The dc voltage was applied with a high-voltage supply through a big resistor (10 MΩ) in order to limit the damage to the sample holder and electrode leads in case of a spark. RF sources could also be connected to these electrodes in order to modulate the molecular transition frequency.[24] The polarization of the laser was lying along one of the axes of the polarization-preserving fiber. Therefore, it was lying in the fiber cleavage plane, similar to the Stark field, but the angle between the two fields is unknown. The measurement of the Stark shift of single molecule lines proceeded as follows: the spectral position of the single molecule's line was first measured in zero field, second under a short series of applied voltages, third in zero field again. With this procedure, the linear part of the laser drift, which was small during the short recording time (a few MHz in about 1 min), was eliminated. For most of the molecules studied, no spontaneous or photoinduced spectral diffusion could be detected.

3. Results and Discussion

The orders of magnitude of the dipole moments and hyperpolarizabilities of usual aromatic molecules indicate that, for reasonable static fields, only linear and quadratic Stark effects can be observed. Indeed, most of the single DBATT molecules we studied in naphthalene and *n*-hexadecane matrixes obeyed the simple relation (1), with linear and quadratic components of the Stark shift. A typical example is presented in Figure 2

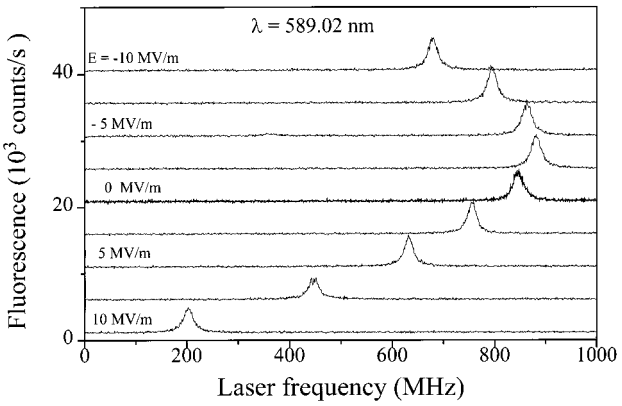

Figure 2. Example of a single molecule line with linear and quadratic Stark shifts (here DBATT in hexadecane at 2 K. The bold line spectrum was recorded at $E = 0$). The linear component around $E = 0$ shows that the central symmetry of the molecule has been broken by the matrix.

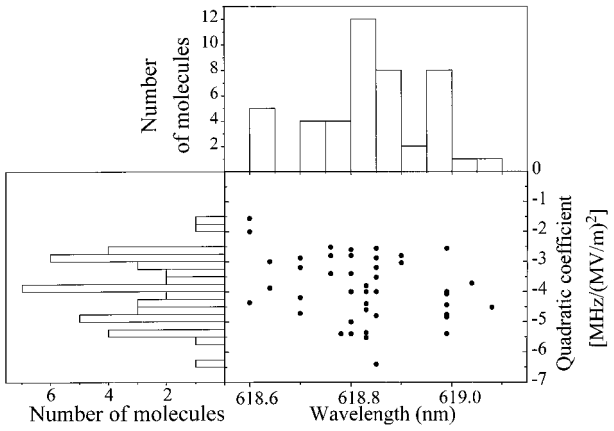

Figure 3. Correlation plot and associated histograms for wavelengths and quadratic *b* coefficients for 43 DBATT molecules in a naphthalene polycrystal. No clear correlation appears between wavelength and *b* coefficient.

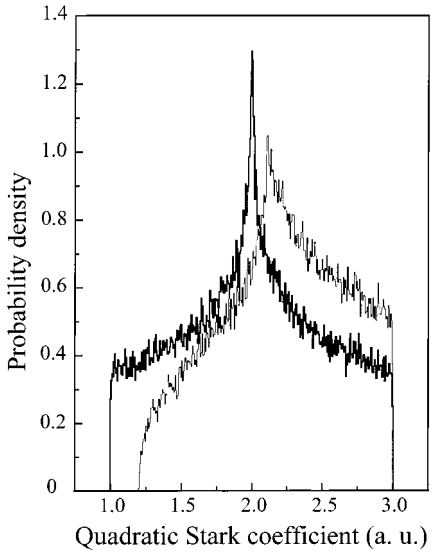

Figure 4. Bold line plot: Histogram of quadratic coefficients obtained by Monte Carlo simulation for an isotropic distribution of molecules. The principal values of the polarizability tensor are 1, 2, and 3 in arbitrary units. The thin-line histogram has been obtained by retaining only the molecules whose squared projection of the transition dipole moment on the laser polarization is larger than 0.1. The laser polarization was supposed to be parallel to the static field, and the transition moment was supposed to be aligned with the large-polarizability axis. Note the shift of the lower cutoff and of the central singularity of the thin-line histogram.

for a DBATT molecule in *n*-hexadecane. The shift varies parabolically as a function of the electric field, and, for the molecule and the maximum field used here, the linear term is of the same order of magnitude as the quadratic one. For a few molecules, we found strong deviations from expression (1). These special cases will be discussed in section 3.2. For the other molecules, the Stark coefficients *a* and *b* can be related to the difference in dipole moment and in polarizability of the molecule between ground and excited electronic states. We have to stress that the dipole moment and polarizability involved here are those of the 'supermolecule', i.e., the probe molecule together with a more or less extended cage of neighboring matrix molecules. If the electronic excitation causes significant changes in the molecular neighborhood, these quantities can be quite different from those of the isolated molecule. In the following, we discuss in separate paragraphs the cases of DBATT in naphthalene and in hexadecane.

3.1. DBATT in Naphthalene. The spectra of the bulk system DBATT in naphthalene have been reported in ref 20. The insertion site of DBATT in the naphthalene crystal is not known, but from sheer volume considerations, the DBATT molecule should replace at least 3 naphthalene molecules in the crystal lattice. The Stark shift was mainly quadratic for all the molecules studied. A statistical correlation plot, together with the histograms of the absorption wavelengths and of the quadratic *b* coefficients for the molecules studied are presented in Figure 3. As is the case in many hole-burning experiments, no clear correlation is found between the position of the line in the inhomogeneous band and the value of the *b* coefficient. The wavelength histogram is consistent with the inhomogeneous distribution of ref 20. The histogram of *b* coefficients is spread in the range between -6 and -1.5 MHz/(MV/m)^2. Taking into account a local field correction factor of 1.7, obtained by averaging isotropic Lorentz factors for the three principal indices of the naphthalene crystal,[25] we obtain polarizability changes ranging between (17 and 68) $\times$ 10^{-40} F m^2 (15 and 61 Å^3). The linear *a* coefficients were often too small to measure. In the few cases where the *a* coefficient was large enough to appear in the fit, its value was less than 10 MHz/(MV/m), corresponding to 6.0 $\times$ 10^{-33} C m (1.5 mD). The order of magnitude of the *a* coefficient values is comparable to the values measured by Wild et al. in pentacene in *p* terphenyl,[16] another crystalline system with inversion symmetry for host and guest. Here again, we may assume that crystal defects in the molecular neighborhoods lead to a slight breaking of the inversion symmetry. The low value of the induced dipole moment difference and the relatively low inhomogeneous broadening as compared to the solvent shift are consistent with the assumption that the crystal defects are only slightly distorting the DBATT molecule.

Let us now come back to the shape of the histogram of quadratic *b* coefficients. In our polycrystalline sample, assuming that the crystallite volume is much less than the illuminated volume, we expect variations of the *b* coefficients of different molecules because of their different orientations with respect to the applied electric field. For an isotropic distribution of molecules, and neglecting the effect of the local crystal field, the distribution of the b-coefficient is easy to simulate from the polarization component in a random direction. Such a simulation is shown by the bold-line histogram of Figure 4 for three arbitrary principal values (here equal to 1, 2, and 3) of the polarizability tensor. The bold histogram of Figure 4 shows three singularities, related to these principal values: two sharp

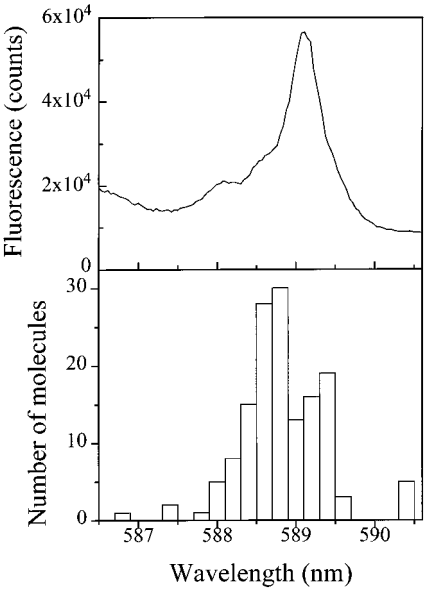

Figure 5. Histogram of the wavelengths of the lines of single DBATT molecules in hexadecane, compared to a bulk fluorescence excitation spectrum of the same system (upper part). Single molecules are found in the main site at 589 nm, but not in the band at 586.5 nm.

edges for the lowest and largest polarizability and a logarithmic divergence related to the intermediate value. It might thus seem possible to deduce these three principal values from a histogram of quadratic *b* coefficients. However, the real histogram is biased by the way we sample single molecules: we detect only those single molecules that have a large enough projection of their transition dipole moment onto the laser polarization. A similar effect in spectral hole burning leads to a deep alteration of the hole shape[12,26,27] as compared to overall distributions of the shifts of all molecules, such as the bold histogram of Figure 4. To account for this effect, we repeated our Monte Carlo simulation, assuming that the transition dipole was lying along the large polarizability axis, and simply eliminated those molecules for which the dipole moment projection on the laser field was too small (squared cosine less than 0.1). This corresponds to a high quality measurement, in which lines 10 times weaker than the maximum intensity are still measurable against the background. The corresponding histogram is shown in thin line in Figure 4. Not only did the lower threshold move with respect to the unbiased histogram, but the position of the intermediate singularity was also shifted. This shows that the parameters of the polarizability tensor are difficult to obtain from the ensemble measurement, even for an ensemble of single molecules. It would be much easier and reliable to follow the position of a single molecule line while varying the direction of the applied field. This, however, is impossible with our present setup.

3.2. DBATT in Hexadecane. Figure 5 shows the wavelength distribution of single DBATT molecule lines around the main site. This histogram is compared to a bulk fluorescence excitation spectrum (Figure 1 of ref 21). Except for the main site at 589 nm, whose shape and width are well reproduced, the shape of the histogram is quite different from that of the spectrum. Much of the structure in the spectrum does not appear in the single molecule histogram and therefore may have a vibronic origin. In particular, we found only very few single molecule lines in the band around 586.5 nm, a structure attributed to another site of DBATT in hexadecane in ref 21.

We obtained the linear and quadratic Stark coefficients for a number of single molecules, by fitting expression (1) to the shifts measured for each molecule and for four values of the voltage.

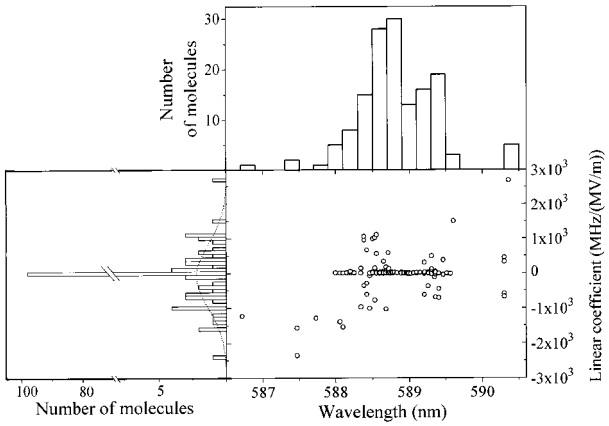

Figure 6. Correlation plot and associated histograms for the wavelengths and the linear a-coefficients for 146 DBATT molecules in hexadecane. Note the large spike at $a = 0$ in the histogram of linear coefficients, although many of the molecules in the main site at 589 nm have not been measured. There is a much broader distribution of *a* coefficients, which also corresponds to a wavelength distribution broader than that of the main site (see text for further details).

Figure 6 shows a correlation plot of the molecular wavelength with the linear *a* coefficient. In the wavelength area of the main site, around 589 nm, the fraction of molecules with a strong a-coefficient was very weak. We therefore did not investigate all the molecules in this frequency area, since most of them had almost purely quadratic Stark shifts (the irregular exploration appears in the wavelengths histogram, in which the main peak is strongly reduced). Nevertheless, we still find a large number of molecules (about 100) with very low *a* coefficients, which were difficult to determine accurately within our experimental frequency resolution. They give the large spike at $a = 0$ in the histogram of the linear Stark coefficients. The width of this spike is about 50 MHz/(MV/m), corresponding to a dipole moment change of $\pm 1.8 \times 10^{-32}$ C m (± 5.5 mD). This value is corrected for a local field factor of 1.4, corresponding to an average refractive index of 1.5 for hexadecane. Again, these dipole moment values are comparable to those of pentacene in *p*-terphenyl or of DBATT in naphthalene. This very narrow a-distribution coexists with a much broader one which has a width of about 3×10^3 MHz/(MV/m), corresponding to a distribution of dipole moment changes between $\pm 1.1 \times 10^{-30}$ C m ($\pm$ 0.3 D). The second *a* distribution is about 60 times broader than the first one. In the plot of Figure 6, there appears to be a gap around 589 nm, the wavelength of the main site, in this second distribution. This is probably only due to our much shallower exploration of this frequency interval, in which the fraction of molecules with a strong a-coefficient was very weak. The striking feature of the *a* histogram is the existence of these two distributions, instead of a single broad one. These two populations have approximately the same center wavelength. Their spectral widths, however, are different, since the fraction of molecules with large linear shifts is much larger in both wings of the general absorption site. In a first interpretation, we may attribute the populations to two sites coinciding at nearly the same wavelength (589 nm), to within 1 nm. These two sites would have central symmetries in the perfect crystal. However, one of them would be much more sensitive to crystal defects than the other, leading to a larger dispersion of *a* coefficients for comparable inhomogeneous widths. As an alternative interpretation, both populations could arise from molecules in the same crystal site, but could correspond to molecules lying either in the bulk of microcrystals or in the disordered boundary areas between microcrystals. The correlation plot indicates no

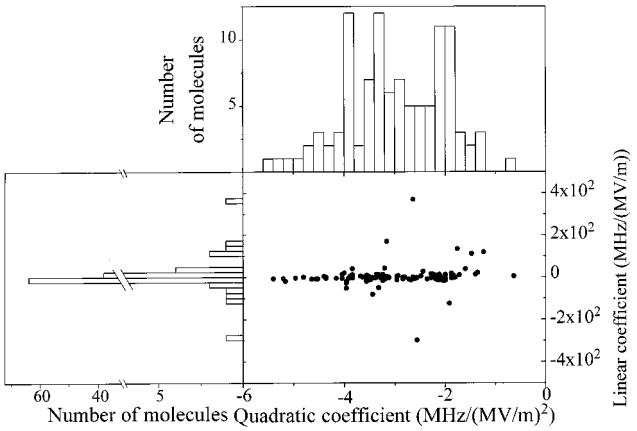

Figure 7. Correlation plot and associated histograms for the linear and quadratic coefficients for 107 DBATT molecules in hexadecane. The quadratic term could not be determined for the molecules of Figure 6 with the largest *a* coefficients. The large linear coefficients seem to be correlated with weak *b* coefficients.

clear relation between wavelength and linear coefficient, except for large shifts from the center wavelength. This must be connected to an anisotropy of the sample, which might arise from a single, or a small number of highly stressed regions in the illuminated spot, presenting a given orientation with respect to the applied electric field.

The histogram of the quadratic *b* coefficients and their correlation with the linear coefficients is shown in Figure 7. The values of the *b* coefficients are distributed between −1.2 and −5.5 MHz/(MV/m)^2, corresponding to polarizability changes varying between (20 and 92) × 10^{-40} F m^2 (18 and 83 Å^3). These values are quite consistent with those measured in naphthalene, taking into account the large inaccuracy in the distance between the electrodes (we used different electrodes for the two samples), and the uncertainty about local field corrections in naphthalene. The general shape of the histogram is also very similar to that of DBATT in naphthalene, which supports our attribution of the distribution to the different orientations of a strongly anisotropic polarizability tensor of the DBATT molecule. Let us now consider the correlation between *a* and *b* coefficients. When the *a* coefficient is large, the quadratic coefficient is difficult to measure accurately. This is why points from the molecules with the strongest *a* coefficients have disappeared from the correlation plot of Figure 7. Nevertheless, there appears to be an excess of molecules with large linear coefficients for low quadratic coefficients (between −1 and −3 MHz/(MV/m)^2). This correlation would be easily explained if the dipole moment difference was oriented mainly perpendicular to the large polarizability axis. No clear correlation between linear and quadratic coefficients is seen for the spiked distribution (i.e., the nearly flat cloud of points in Figure 7).

For some rare molecules, two or three in the 200 molecules or so we studied, the shift could not be fitted using the form 1. Similar deviations from a second degree polynomial were also observed for terrylene in *p*-terphenyl.[18] A particularly striking example, which we will discuss in some detail, is displayed in Figure 8. For the molecule of Figure 8, the shift as a function of the electric field can be represented as the sum of a linear term and of a cubic term. The lower plot of Figure 8 shows the residual shifts after a linear fit has been subtracted from the data. This residual is seen to be an odd function of the electric field, and is almost perfectly fitted by a cubic power. It was not possible to determine a quadratic term for this molecule within our experimental accuracy. Note that the order of magnitude of the quadratic term measured for "normal" DBATT

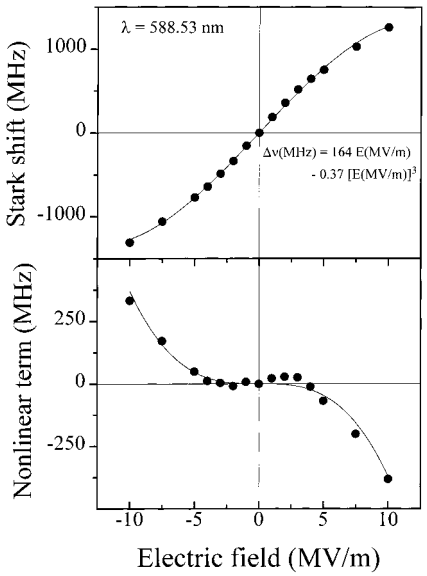

Figure 8. Upper part: Stark shift of a peculiar single DBATT molecule in hexadecane, for which no second order polynomial could fit the data. Lower part: After subtraction of the best linear fit, the residual can be perfectly fitted with a cubic variation. Such a dependence cannot be explained in terms of constant dipole moment and polarizability.

molecules (see Figure 7) is comparable to that of the cubic term of Figure 8.

We now discuss possible explanations for the observed field dependence. As discussed in the Introduction, the contribution of the second-order polarizability $\chi^{(2)}$, which would give a third-order term in the energy, should be negligible as compared to the quadratic term arising from the first order (ordinary) polarizability. $\chi^{(2)}$ is further reduced because in the centrosymmetric DBATT molecule it is induced by perturbations from the nonsymmetric matrix cage. Since even the effect of the first order polarizability is not visible in Figure 8, it is very unlikely that the term due to the second-order polarizability could contribute significantly.

The purely electronic Stark effect of a rigid molecule with fixed and largely spaced energy levels can hardly explain the data of Figure 8. Assuming that the geometry of the molecule (or of the supermolecule) can change with electric field, the dipole moment and first-order polarizability can depend on electric field, leading to deviations from expression (1). To obtain a third-order term in the energy, the dipole moment must have a quadratic dependence on *E*, or the polarizability must have a linear dependence on *E*. Here, we propose a simple model for a quadratic dependence of the dipole moment change with the applied electric field. The molecule of Figure 8 has a permanent dipole moment change $\delta\vec{\mu}$, which is induced by noncentrosymmetric surroundings in the matrix. Since this dipole moment depends on molecular positions around the molecule to the first order, it also depends on pressure p to the first order:

$$\delta\vec{\mu} = \delta\vec{\mu}_0 + \vec{k}p \tag{3}$$

Now, an applied electric field exerts an electrostrictive pressure:

$$p_e = (\epsilon_r - 1)\epsilon_0 E^2/2 \tag{4}$$

The shift due to this electrostrictive pressure is usually about 10 times weaker than the polarizability shift.[28] However, the molecule of Figure 8 could be highly sensitive to pressure. Indeed, large fluctuations of the pressure shift of single molecule lines can be found even in crystalline samples.[29] The pressure

shift could explain the quadratic change in polarization and therefore the cubic energy shift. Unfortunately, when the experiment was done, we did not measure the pressure dependence of the transition frequency. Other complex behaviors can be expected for molecules located near crystal defects, because of the highly nonharmonic form of intermolecular potentials there. For example, if a two-level system[30,31] is affected by the applied field, an electric field-driven jump could lead to discontinuities and slope changes in the field curve.[18]

4. Conclusion

In this work, we investigated the Stark effect on single DBATT molecules in a naphthalene crystal, where it is quadratic, and in an *n*-hexadecane Shpol'skii matrix, where it has linear and quadratic components. In the hexadecane matrix, strong linear coefficients are dominantly found in the wings of the main site, while molecules in the center of the site are dominantly quadratic. On the basis of the histogram of linear coefficients, we attributed this feature to two distinct populations of molecules. For one of those, the molecules are very sensitive to, or located near crystal defects. As has already been observed by hole burning, the insertion site bears a strong influence on the induced dipole moment of a guest molecule, and therefore on the linear part of its Stark effect. For the centrosymmetric environment of naphthalene, and for one of the populations in hexadecane, the induced dipole moments are less than a few mD, of an order of magnitude comparable to that of pentacene in *p*-terphenyl.[16] The quadratic coefficients were also found to be broadly distributed between a maximal and a minimal value about 4 times lower. These differences were attributed to the anisotropy of the polarizability tensor, probed by different orientations of the molecules in the polycrystalline samples with respect to the applied field. We showed, with a simple Monte Carlo simulation, that finding the three polarizability components from the experimental histogram is difficult because of the bias introduced by the optical selection of single molecules. For each particular site, the data showed no significant statistical correlations of the Stark parameters with wavelength. However, quadratic and linear coefficients may be linked through the orientation of the induced dipole moment and of the polarizability tensor with respect to the molecular axes. Some rare molecules had Stark shift components that were neither linear nor quadratic in electric field. We attribute such behaviors to molecules close to defects, where the application of an electric field can lead to significant geometrical changes in the molecule or in the supermolecule.

Acknowledgment. We are very grateful to Prof. Th. Basché and to F. Kulzer for providing unpublished data on the Stark effect of terrylene in *p*-terphenyl. We also thank Dr. R. Brown and P. Bordat for stimulating discussions. This work was supported by Ultimatech (CNRS), Région Aquitaine, and by a grant from the German Academic Exchange Service, DAAD, for J.C.W.

References and Notes

(1) Labhart, L. *Adv. Chem. Phys.* **1967**, *3*, 179. Liptay, W. In *Excited States*; Lim, E. C., Ed.; Academic: New York, 1974; Vol. 1.

(2) For example, see: Blinov L. M. *Sov. Sci. Rev. A Phys. Rev.* **1989**, *12*, 1. Grewer, G.; Lösche, M. *Thin Solid Films* **1992**, *210/211*, 670.

(3) Meyling, J. H.; Hesselink, W. H.; Wiersma, D. A. *Chem. Phys.* **1976**, *17*, 353.

(4) Moerner, W. E., Ed. *Persistent Spectral Hole Burning: Science and Applications*; Springer: Berlin, 1988.

(5) Orrit, M.; Bernard, J.; Personov, R. I. *J. Phys. Chem.* **1993**, *97*, 10256.

(6) Marchetti, A. P.; Scozzafava, M.; Young, R. H. *Chem. Phys. Lett.* **1977**, *51*, 424.

(7) Burkhalter, F. A.; Suter, G. W.; Wild, U. P.; Samoilenko, V. D.; Rasumova, N. V.; Personov, R. I. *Chem. Phys. Lett.* **1983**, *94*, 483.

(8) Kohler, B. E.; Personov, R. I.; Woehl, J. C. In Laser Techniques in Chemistry; Rizzo, Th., Myers, A., Eds.; John Wiley & Sons: New York, 1984.

(9) Gradl, G., Kohler, B. E., Westerfield, C. *J. Chem. Phys.* **1992**, *97*, 6064.

(10) Geissinger, P.; Kohler, B. E.; Woehl, J. C. *J. Phys. Chem.* **1995**, *99*, 16527; Geissinger, P.; Kohler, B. E., Woehl, J. C. *Synth. Met.* **1997**, *84*, 937.

(11) Kohler B. E.; Woehl, J. C. *J. Chem. Phys.* **1995**, *102*, 7773; *J. Chem. Phys.* **1996**, *104*, 3148.

(12) Kador, L.; Haarer, D.; Personov, R. I. *J. Chem. Phys.* **1987**, *86*, 5300.

(13) Munn, R. W. *Chem. Phys.* **1998**, *236*, 151.

(14) Shen, Y. R. *The Principles of Nonlinear Optics*; Wiley: New York, 1984; p 13.

(15) An order of magnitude of the polarizability is given by the square of the transition dipole moment μ_t divided by the energy difference ΔE between ground and first excited levels. A similar estimation of $\chi^{(2)}$ shows that the ratio of the cubic to quadratic terms in the energy is of the order of E/E_{mol}, $E_{mol} = \Delta E/\mu_t$ being a typical value of the electric field acting within the molecule.

(16) Wild, U. P.; Güttler, Pirotta, F. M.; Renn, A. *Chem. Phys. Lett.* **1992**, *193*, 451.

(17) Orrit, M.; Bernard, J.; Zumbusch, A.; Personov, R. I. *Chem. Phys. Lett.* **1992**, *196*, 595.

(18) Kulzer, F. Ph.D. Thesis, 1998. In preparation.

(19) Kummer, S.; Basché, T.; Bräuchle, C. *Chem. Phys. Lett.* **1994**, *229*, 309; **1995**, *232*, 414.

(20) Jelezko, F.; Lounis, B.; Orrit, M. *J. Chem. Phys.* **1997**, *107*, 1692.

(21) Boiron, A.-M.; Lounis, B.; Orrit, M. *J. Chem. Phys.* **1996**, *105*, 3969.

(22) For example, see: Orrit, M.; Bernard, J.; Brown, R.; Lounis, B. In *Progress in Optics*; Wolf, E., Ed., Elsevier Science, New York, 1996, p 61.

(23) Representing the electrodes of Figure 1 by two thin, infinite, and conducting half-plates, one can calculate the field in the gap exactly with the coordinates of the elliptical cylinder. The field at the center is $2/\pi \times V/d$, V being the applied voltage and d the distance between the electrodes.

(24) Brunel, Ch.; Lounis, B.; Tamarat, Ph.; Orrit, M. *Phys. Rev. Lett.* **1998**, *81*, 2679.

(25) Winchell, A. N. *The Optical Properties of Organic Compounds*; Academic Press: New York, 1954; p 77.

(26) Meixner, A. J.; Renn, A.; Bucher, S. E.; Wild, U. P. *J. Phys. Chem.* **1986**, *90*, 6777.

(27) Maier, M. *Appl. Phys. B* **1986**, *41*, 73.

(28) Plakhotnik, T.; Walser, D.; Renn, A.; Wild, U. P. *Phys. Rev. Lett.* **1996**, *77*, 5365.

(29) Müller, A.; Richter, W.; Kador, L. *Chem. Phys. Lett.* **1995**, *241*, 547.

(30) Brown, R.; Orrit, M. In Single Molecule Optical Detection, Imaging, and Spectroscopy; Basché, Th., Moerner, W. E.; Orrit, M.; Wild, U. P. VCH Weinheim, Germany, 1997.

(31) Reilly, P. D.; Skinner, J. L. *J. Chem. Phys.* **1995**, *102*, 1540.